

Stability Analysis and Adaptive Control Design of Multi-Converter-Based Systems With STATCOMs Under Varying Operating Conditions

Hui Yuan, Huanhai Xin, Linbin Huang, Di Zheng

Abstract—The increasing penetration of converter-based renewables (CBRs) synchronizing with grids through phase-lock loops (PLLs) is challenging the secure grid operations. In such a power system, the strong interaction among CBRs and power network may cause small-signal stability issues, especially in low short-circuit grids. Besides, the integration of static synchronous compensators (STATCOMs) in a multi-CBR system for voltage support may deteriorate the small-signal stability. However, it is challenging to assess the small-signal stability and ensure the robust stability of such a multi-CBR system with STATCOMs due to the complex system dynamics and varying operating conditions. To tackle the challenges, this paper proposes a novel method for small-signal stability assessment of a multi-CBR system with STATCOMs from the viewpoint of grid strength, which can consider the varying operating conditions. Based on the proposed grid-strength-based method, we find the *critical operating conditions*, wherein the system tends to be most unstable. On this basis, the robust small-signal stability issues of the multi-CBR system with STATCOMs can be simplified as that of multiple subsystems under *critical operating conditions*, which can avoid establishing detailed models of the original system and considering all operating conditions. Moreover, an adaptive control-parameter design method is proposed for STATCOMs to ensure the robust small-signal stability of the multiple subsystems under *critical operating conditions*. The efficacy of the proposed methods is validated by a 39-node test system.

Index Terms—converter, STATCOMs, small-signal stability, grid strength, adaptive control.

I. INTRODUCTION

The increasing penetration of renewable resources, commonly interfacing with ac grids through power converters, is changing the modern power system dynamics and challenging the stable grid operations^{[1],[2]}. Particularly, the converter-based renewables (CBRs) with widely-used grid-following controls tracking the grid frequency through phase-lock loops (PLLs) may cause sub/sup-synchronous oscillation issues due to the strong interaction between fast dynamics of CBRs and grid network, especially in low short-circuit grids^{[3]-[7]}. Besides, in practical wind farms and photovoltaic plants, the static synchronous compensator (STATCOM) is commonly required for reactive power compensation. However, the STATCOMs may interact with CBRs and thus deteriorate

CBR-induced oscillation issues^{[8]-[10]}. For instance, in 2015, a sub-synchronous resonance event was recorded in the wind farm with STATCOMs in Hami, China.

To understand the mechanism and characteristics of the CBR-induced oscillation issues, many small-signal stability analysis methods have been proposed, mainly consisting of eigenvalue analysis method^[11], and impedance-based analysis method^{[9],[12]-[15]}. Since the impedance-based analysis method does not need the detailed parameters of CBRs, which uses the input-output impedance of the CBRs and network to analyze the small-signal stability, the impedance-based analysis method has been widely used. For instance, Ref. [12] derived two single-input single-output models (SISO) by ignoring the off-diagonal elements of the impedance matrix for a single-CBR infinite-bus system, and analyzed the small-signal stability by Nyquist stability criterion. However, this simplification may cause the inaccuracy of stability analysis results. To deal with this issue, Ref. [13] derived the improved SISO model of the system and analyzed the impact of the PLL's bandwidth on the small-signal stability, which considered the off-diagonal elements of the impedance matrix. Ref. [14] derived a novel SISO model, which can not only consider the off-diagonal elements of the impedance matrix, but also revealed the CBR-induced oscillation characteristic from the viewpoint of circuit. These previous works focus on the small-signal stability analysis of a single-CBR infinite-bus system. To analyze the impacts of the interaction between STATCOMs and CBRs on the small-signal stability, Ref. [9] established the sequence impedance of a wind farm with a STATCOM and evaluated the damping provided by the STATCOM. The impedance-based analysis method commonly used the Nyquist stability criterion for small-signal stability analysis, which is based on the reduced SISO transfer function of the system with the assumption that it has no right-half-plane pole. However, this assumption is not always satisfied^[15]. To overcome this drawback, Ref. [10] furtherly proposed a generalized short-circuit ratio (gSCR)-based method to evaluate the small-signal stability margin of a multi-CBR system with STATCOMs under the rated operating condition from the viewpoint of grid strength. However, few works have investigated the small signal stability of a multi-CBR system with STATCOMs under varying operating conditions.

To suppress the CBR-induced oscillation issues, many works proposed improved control design strategies, which can be divided into two categories: the control design of CBRs^[16] and the control design of additional devices (e.g., energy-storage devices^[17] or STATCOMs^[9]). For instance, Ref.

H. Yuan, H. Xin are with the college of electrical engineering, Zhejiang university, Hangzhou 310027, China (e-mail: yuan_hui@zju.edu.cn; xinhh@zju.edu.cn);

Linbin Huang is with the Department of Information Technology and Electrical Engineering, ETH Zürich, 8092 Zürich, Switzerland (e-mail:linhuang@ethz.ch).

[16] proposed a PLL-resaping method to improve the small-signal stability of a single-CBR infinite-bus system. However, the CBR is commonly packaged and thus it is hard to adjust the CBR's inner control parameters in practical operations. In comparison, the STATCOM is "white-boxed" model and thus it is more convenient to adjust the STATCOM's control parameters. For instance, Ref. [9] proposed an intelligent parameter design method for STATCOMs to mitigate the resonance in wind farms, which is based on the gain margin or phase margin of the reduced SISO transfer function of the system. However, this method may be ineffective if the obtained SISO transfer function has the right-half-plane pole. Ref. [17] proposed an enhancing grid stiffness control strategy of STATCOMs, which shapes the impedance of STATCOMs as inductances and improves the system stability by increasing the grid strength or short-circuit ratio (SCR). These previous works only focused on one certain operating condition, which cannot ensure the stability of the system under varying operating conditions.

To suppress the oscillation issues of wind farms under varying operating conditions in weak grids, this paper proposes an adaptive control parameter design method for STATCOMs. We firstly propose a grid-strength-based method for evaluating small-signal stability margin of the multi-CBR with STATCOMs under varying operating conditions, which was the extension of our previous work for stability analysis of the multi-CBR system with STATCOMs under the rated operating condition. The proposed method can simplify the small-signal stability analysis of the multi-CBR system with STATCOMs as that of multiple subsystems from the viewpoint of grid strength, which avoids deriving the detailed model of the original system. Besides, based on the proposed method, we find the *critical* operating conditions, wherein the multi-CBR system with STATCOMs tends to be most unstable. In other words, if the multi-CBR system with STATCOMs is stable under *critical* operating conditions, then the system is also stable under other operating conditions. This can highly simplify the difficulty of robust small-signal stability issues of the multi-CBR system with STATCOMs under varying operating conditions. On this basis, we propose an adaptive control parameter design method for STATCOMs to ensure robust small-signal stability of the established multiple subsystems under *critical* operating conditions, which is robustly effective for the original system under varying operating conditions. The main contributions of this paper can be summarized as

1) It is proved that a multi-CBR system with STATCOMs under varying operating conditions can be converted as multiple subsystems for small-signal stability analysis. On this basis, a grid-strength-based method is proposed to evaluate the stability margin of the multi-CBR system with STATCOMs under varying operating conditions. This proposed method can highly simplify the difficulty of small-signal stability assessment by avoiding modelling the detailed dynamics of the multi-CBR system with STATCOMs.

2) On this foundation, it is derived that the robust small-signal stability issue of a multi-CBR system with STATCOMs under varying operating conditions can be converted to that of

multiple subsystems under *critical* operating conditions, wherein the system tends to be unstable. This can highly simplify the robust small-signal stability issues of a multi-CBR system with STATCOMs, which does not need to consider all operating conditions and establish the detailed system model.

3) Based on the H_∞ control theory^[18], an adaptive control parameter design method is proposed for STATCOMs to ensure the robust small-signal stability of the established subsystems under *critical* operating conditions. It is verified that the proposed adaptive control parameter method can ensure the robust stability of the multi-CBR system with STATCOMs under varying operating conditions, even that the CBRs are "black-box" models.

The rest of this paper is organized as follows. Section II describes the dynamic model of the multi-CBR system with STATCOMs under varying operating conditions and the focused issues. In section III, a grid-strength-based method is proposed for small-signal stability assessment of the multi-CBR system with STATCOMs under varying operating conditions. Section IV proposes an adaptive control parameter design method for STATCOMs. In Section V, the efficacy of the proposed methods is demonstrated by eigenvalue analysis and time-domain simulations on a 39-node system. In section VI, the conclusions are drawn.

II. SYSTEM MODELING AND PROBLEM DESCRIPTION

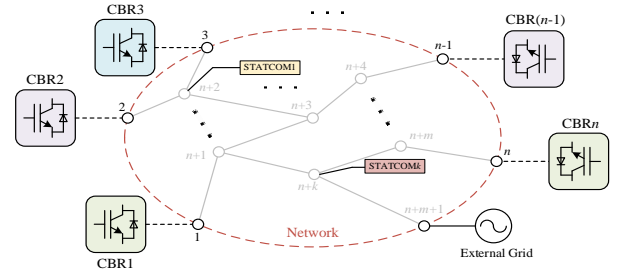


Fig. 1 One-line diagram of a typical multi-CBR system with STATCOMs.

Let us consider a multi-CBR system with k STATCOMs as shown in Fig. 1, where nodes $1 \sim n$ are connected to CBRs, node $n+m+1$ is connected to external grids (simplified as the ideal voltage source); the remaining nodes are passive nodes. Since in practical grids the STATCOMs are not directly connected to CBRs' terminal nodes, here we assume that STATCOM1~STATCOM k are connected to the passive nodes $n+1 \sim n+k$. To simplify the analysis, in the following we assume that the STATCOMs are all applied with the ac-voltage control (AVC) and the control parameters of STATCOMs are identical; besides, the AVC of STATCOMs is not saturated, i.e., the reactive current reference I_{qref} is in the range of $[-1, 1]$.

When the system operates on non-rated conditions, the closed-loop characteristic equation of the multi-CBR system with STATCOMs is expressed as (1), which can be used for small-signal stability analysis:

$$\det(\mathbf{Y}_{Gm}(s) + \mathbf{Y}_{Nm}(s)) = 0 \quad (1)$$

$$\mathbf{Y}_{Gm}(s) = \begin{bmatrix} \text{diag}(\mathbf{Y}'_{CBR_i}(s)) & \\ & \text{diag}(\mathbf{Y}'_{STATCOM_j}(s)) \end{bmatrix} \quad (2)$$

$$\begin{cases} \mathbf{Y}'_{\text{CBR}i}(s) = P_{ei} \mathbf{Y}_{\text{CBR}i}(s), i = 1, \dots, n \\ \mathbf{Y}'_{\text{STA}j}(s) = S_{Bsj} \mathbf{Y}_{\text{STA}j}(s), j = n+1, \dots, n+k \end{cases} \quad (3)$$

$$\mathbf{Y}_{\text{STA}j}(s) = \begin{bmatrix} Y_{11}(s) & I_{qj} \tilde{Y}_{12}(s) \\ Y_{21}(s) & Y_{22}(s) \end{bmatrix} \quad (4)$$

$$\begin{cases} Y_{11}(s) = \frac{C_{dcs}s}{(H_{is}(s) + sL_{fs})C_{dcs}s + H_{is}(s)H_{dcs}(s)} \\ \tilde{Y}_{12}(s) = \frac{Y'_{12}(s) + H_{plls}(s)}{1 + H_{plls}(s)} \\ Y_{21}(s) = -\frac{H_{is}(s)H_{acs}(s)}{sL_{fs} + H_{is}(s)} \\ Y_{22}(s) = \frac{1}{(1 + H_{plls}(s))(H_{is}(s) + sL_{fs})} \\ Y'_{12}(s) = \frac{H_{is}(s)H_{dcs}(s) - C_{dcs}L_{fs}s^2H_{plls}(s)}{(H_{is}(s) + sL_{fs})C_{dcs}s + UH_{is}(s)H_{dcs}(s)} \end{cases} \quad (5)$$

$$\mathbf{Y}_{Nm}(s) = \mathbf{B}_{red} \otimes \boldsymbol{\gamma}(s) = \begin{bmatrix} \mathbf{B}_{11} & \mathbf{B}_{12} \\ \mathbf{B}_{21} & \mathbf{B}_{22} \end{bmatrix} \otimes \boldsymbol{\gamma}(s) \quad (6)$$

$$\boldsymbol{\gamma}(s) = \frac{1}{(s + \tau)^2 / \omega_0 + \omega_0} \begin{bmatrix} (s + \tau) & \omega_0 \\ -\omega_0 & (s + \tau) \end{bmatrix} \quad (7)$$

where $\mathbf{Y}_{Gm}(s)$ and $\mathbf{Y}_{Nm}(s)$ represent the admittance matrices of the devices and network, respectively; $\mathbf{Y}'_{\text{CBR}i}(s)$ and $\mathbf{Y}'_{\text{STA}j}(s)$ are admittance matrices of CBR*i* and STATCOM*j*, respectively, the detailed derivation of which refers to Ref. [19] and [20]; P_{ei} and S_{Bsj} are the active power output of CBR*i* and the rated capacity of STATCOM*j*; $\mathbf{Y}_{\text{CBR}i}(s)$ and $\mathbf{Y}_{\text{STA}j}(s)$ are admittance matrices of CBR*i* and STATCOM*j* normalized at their rated capacities, respectively; the description of STATCOMs' parameters in (5) refer to TABLE III; $\mathbf{B}_{red} \in \mathbf{R}^{(n+k) \times (n+k)}$ is the node-reduced susceptance matrix of the network containing the CBRs' nodes and STATCOMs' nodes; $\mathbf{B}_{11} \in \mathbf{R}^{n \times n}$, $\mathbf{B}_{12} \in \mathbf{R}^{n \times k}$, $\mathbf{B}_{21} \in \mathbf{R}^{k \times n}$, $\mathbf{B}_{22} \in \mathbf{R}^{k \times k}$ are submatrices of \mathbf{B}_{red} ; $\tau = R/L$ represents the ratio of resistor (R) to inductance (L) of the network line. Here we assume that all network lines have the same ratio τ ; ω_0 is the rated synchronous frequency.

By submitting (2) and (6) into (1), the closed-loop characteristic equation (1) can be written as:

$$\det \left(\begin{bmatrix} \text{diag}(P_{ei} \mathbf{G}_{\text{CBR}i}(s)) & \\ & \text{diag}(S_{Bsj} \mathbf{G}_{\text{STA}j}(s)) \end{bmatrix} + \mathbf{B}_{red} \otimes \boldsymbol{\gamma}(s) \right) = 0 \quad (8)$$

We can see from (8) that the CBRs interact with STATCOMs through the network, which may cause small-signal stability issues, especially in weak grids. To this end, this paper mainly focuses on addressing two issues:

- 1) How to evaluate small-signal stability of the multi-CBR system with STATCOMs under varying operating conditions?
- 2) How to design the control parameters of STATCOMs to ensure the robust small-signal stability of the system under varying operating conditions?

For *issue 1*, we can see from (8) that it is challenging to directly solve the characteristic equation (8) for small-signal stability analysis because of the complex interactions among

CBRs and STATCOMs through the network, especially considering varying operating conditions. To deal with this issue, a method will be proposed in Section III from the viewpoint of grid strength. For *issue 2*, an adaptive parameter design method for STATCOMs will be proposed in Section IV.

III. SMALL-SIGNAL STABILITY ANALYSIS OF MULTI-CBR SYSTEM WITH STATCOMS UNDER VARYING OPERATING CONDITIONS

A. Proposed Grid-Strength-Based Method

In our previous work^[10], we proposed a generalized short circuit ratio (gSCR)-based method to evaluate the small-signal stability of a multi-CBR system with STATCOMs under the rated operating condition. To be special, we convert the multi-CBR system with STATCOMs into a multi-STATCOM system and an equivalent homogeneous system for small-signal stability analysis. With the assumption that the multi-STATCOM system is stable, the small-signal stability of the multi-CBR system with STATCOMs can be represented by the established equivalent homogeneous system. The equivalent homogeneous system can be furtherly decoupled into n independent subsystems for small-signal stability analysis, wherein these subsystems have the same equivalent device but different SCRs. Due to this, the small-signal stability of the equivalent homogeneous system (or the original system) can be represented by the *critical* subsystem with the smallest SCR, (named as generalized short-circuit ratio, gSCR). The expression of gSCR is given as:

$$\text{gSCR} = \lambda_{\min} \{ \mathbf{S}_B^{-1} \mathbf{B}_{redn} \}, \mathbf{S}_B = \text{diag} \{ S_{Bi} \}, \mathbf{B}_{redn} = \mathbf{B}_{11} - \mathbf{B}_{12} \mathbf{B}_{22}^{-1} \mathbf{B}_{21} \quad (9)$$

where $\lambda_{\min} \{ \}$ denotes the smallest eigenvalue of a matrix; \mathbf{S}_B is a diagonal matrix, wherein the diagonal element S_{Bi} is the rated capacity of CBR*i*; \mathbf{B}_{11} , \mathbf{B}_{12} , \mathbf{B}_{21} and \mathbf{B}_{22} refer to (6).

When the control parameters of CBRs and STATCOMs are given, gSCR can be used to quantify the small-signal stability margin of the multi-CBR system with STATCOMs under the rated operating condition. The characteristic equation of the multi-CBR system with STATCOMs under the rated operating condition is given as:

$$\det \left(\begin{bmatrix} \text{diag}(S_{Bi} \mathbf{G}_{\text{CBR}i}(s)) & \\ & \text{diag}(S_{Bsj} \mathbf{G}_{\text{STA}j}(s)) \end{bmatrix} + \mathbf{B}_{red} \otimes \boldsymbol{\gamma}(s) \right) = 0 \quad (10)$$

We can see from (8) and (10) that the multi-CBR system with STATCOMs under non-rated operating conditions has a similar characteristic equation as the system under the rated operating condition. Therefore, referring to [10], the small-signal stability of the multi-CBR system with STATCOMs under non-rated operating conditions can also be represented by an equivalent homogeneous system and its decoupled *critical* subsystem, as shown in Fig. 2. The characteristic equation of the decoupled *critical* subsystem is given as^[10]:

$$\det(\mathbf{C}_1(s)) = \det(\bar{\mathbf{Y}}_s(s) \boldsymbol{\gamma}^{-1}(s) + \lambda_1 \mathbf{I}_1) = 0, \lambda_1 = \lambda_{\min} \{ \mathbf{P}_e^{-1} \mathbf{B}_{redn} \} \quad (11)$$

$$\bar{\mathbf{Y}}_s(s) = \bar{\mathbf{Y}}_{\text{CBR}}(s) + \bar{\mathbf{Y}}_{\text{STA}}(s) \quad (12)$$

$$\bar{\mathbf{Y}}_{\text{CBR}}(s) = \sum_{i=1}^n p_{1i} \mathbf{Y}_{\text{CBR}i}(s), \bar{\mathbf{Y}}_{\text{STA}}(s) = \sum_{j=n+1}^{n+k} p_{2j} \mathbf{Y}_{\text{STA}j}(s) \quad (13)$$

$$p_{1i} = v_{1i} u_{1i}, \quad p_{2j} = S_{Bsj} \bar{u}_1^T \begin{bmatrix} \mathbf{P}_e^{-1} \\ \mathbf{I}_k \end{bmatrix} \mathbf{E}_{sj} \bar{v}_1 \quad (14)$$

$$\bar{u}_1^T = \begin{bmatrix} u_1^T & -u_1^T \mathbf{P}_e^{-1} \mathbf{B}_{12} \mathbf{B}_{22}^{-1} \end{bmatrix}, \quad \bar{v}_1 = \begin{bmatrix} v_1 \\ -\mathbf{B}_{22}^{-1} \mathbf{B}_{21} v_1 \end{bmatrix} \quad (15)$$

where $\mathbf{C}_1(s)$ is the closed-loop transfer function matrix of the *critical* subsystem; $\bar{\mathbf{Y}}_s(s)$ is the device's dynamics, which is the weighted sum of all CBRs and STATCOMs; $\mathbf{P}_e = \text{diag}(P_{ei})$ is a diagonal matrix, wherein the diagonal element P_{ei} is the active power output of CBR i ; p_{1i} ($i=1, \dots, n$) and p_{2j} ($j=n+1, \dots, n+k$) are the participation factors; u_{1i} and v_{1i} are the i th elements of \bar{u}_1^T and \bar{v}_1 ; u_1^T and v_1 are normalized left and right eigenvectors of the smallest eigenvalue λ_1 for $\mathbf{P}_e^{-1} \mathbf{B}_{redn}$; \mathbf{E}_{sj} is a square matrix representing the location of STATCOM j , wherein only the j th diagonal element is one and the other elements are zero. The $\bar{\mathbf{Y}}_{STA}(s)$ is rewritten as (16) under the assumption that the STATCOMs have the same control parameters:

$$\bar{\mathbf{Y}}_{STA}(s) = p_\Sigma \bar{\mathbf{Y}}_{STA1}(s), \quad \bar{\mathbf{Y}}_{STA1}(s) = \begin{bmatrix} Y_{11}(s) & I_{q\Sigma} \bar{Y}_{12}(s) \\ Y_{21}(s) & Y_{22}(s) \end{bmatrix} \quad (16)$$

$$p_\Sigma = \sum_{j=n+1}^{n+k} p_{2j}, \quad I_{q\Sigma} = \frac{\sum_{j=n+1}^{n+k} p_{2j} I_{qsj}}{p_\Sigma} \quad (17)$$

We can see from (16) and (4) that $\bar{\mathbf{Y}}_{STA}(s)$ can be considered as the dynamic of a STATCOM, where p_Σ and $I_{q\Sigma}$ can be considered as the capacity and reactive current output, respectively. Moreover, since $p_{2j} \geq 0$ and I_{qsj} is in the range of $[-1, 1]$, $I_{q\Sigma}$ is in the range of $[-1, 1]$. Thus, the dynamics of the device $\bar{\mathbf{Y}}_s(s)$ in (12) for the equivalent *critical* system can be considered as the weighted sum of CBRs and a STATCOM.

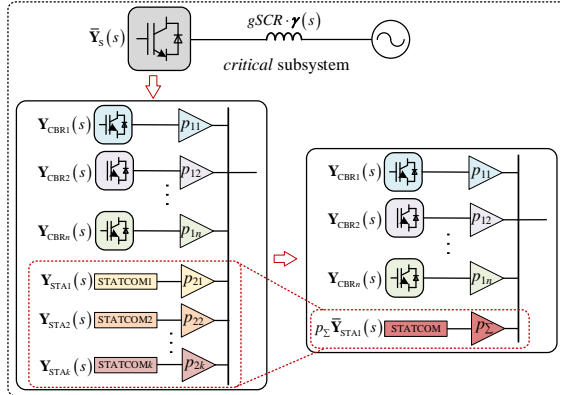


Fig. 2 Diagram of the *critical* subsystem representing small-signal stability of the multi-CBR system with STATCOMs under non-rated operating conditions.

Referring to (9) and (11), we can see that the $gSCR$ and λ_1 have similar definitions. In other words, the $gSCR$ can be extended to evaluate small-signal stability of the multi-CBR system with STATCOMs under non-rated operating conditions, when the control parameters of CBRs and STATCOMs are given. Here, we give the definition of $gSCR$ and its critical value for small-signal stability evaluation of the multi-CBR system with STATCOMs under varying operating conditions.

Definition 1: the $gSCR$ is defined to evaluate the grid strength of the multi-CBR system with STATCOMs under varying operating conditions:

$$gSCR = \lambda_{\min} \{ \mathbf{P}_e^{-1} \mathbf{B}_{redn} \} \quad (18)$$

Definition 2: The *critical* value of $gSCR$ (named as $CgSCR$) is defined to represent that the system is *critically* stable:

$$CgSCR = \arg \left\{ \det \left(\bar{\mathbf{Y}}_s(s_c) \mathbf{Y}^{-1}(s_c) + gSCR \cdot \mathbf{I}_1 \right) \right\} = 0 \quad (19)$$

where $\arg\{\}$ denotes the eigenvalue calculation of $CgSCR$; $s_c = j\omega_c$ is dominant eigenvalues of the *critical* subsystem in (11), which is located at the imaginary axis in complex plane; ω_c is oscillation frequency.

Based on the $gSCR$ and $CgSCR$, we can evaluate the small-signal stability of the multi-CBR system with STATCOMs under varying operating conditions from the viewpoint of grid strength. The detailed features of this proposed grid-strength-based method is given in the following subsection.

B. Features of Proposed Grid-Strength-Based Method

According to the discussion in the above subsection, the grid-strength indicator, i.e., $gSCR$, can not only evaluate the small-signal stability of the multi-CBR system with STATCOMs under rated operating condition, but also under non-rated operating conditions, which has following features:

1) The $gSCR$ can reflect grid strength of the multi-CBR system with STATCOMs under varying operating conditions, similar as the SCR in a single-CBR infinite-bus system. That is, the smaller the $gSCR$ is, the weaker the grid strength is. Besides, in the definition of $gSCR$, the rated operating condition can be considered as a special case. In this case, the CBR i 's active power output is equal to the rated capacity (i.e., S_{Bi}) and thus the definition of $gSCR$ in (9) is equivalent to that in (18).

2) The $gSCR$ and $CgSCR$ can be used to evaluate small signal stability margin of the multi-CBR system with STATCOMs under varying operating conditions. That is, if $gSCR > CgSCR$, the system is stable; the larger the ($gSCR - CgSCR$) is, the more stable the system is; otherwise, if $gSCR < CgSCR$, the system is unstable.

3) The connection of STATCOMs has no impact on $gSCR$, but has an impact on $CgSCR$. This is because $gSCR$ is that of the multi-CBR system without STATCOMs as shown in (11), but the calculation of $CgSCR$ is related with the dynamics of STATCOMs as shown in (19). Moreover, the participation factor p_{2j} reflects the relative degree of the impact of STATCOM j on the $CgSCR$ or (system's stability). That is, the larger p_{2j} is, the larger the impact of STATCOM j on $CgSCR$ is.

4) The small-signal stability of the multi-CBR system with STATCOMs under varying operating conditions is bounded by the dynamics of CBRs and STATCOMs. To analyze the small-signal stability of the multi-CBR system with STATCOMs, we define n equivalent subsystems as shown in Fig. 3(b). These n equivalent subsystems have different devices' dynamics, but the same $gSCR$. In each subsystem, the devices include a CBR in the original system and a STATCOM $\bar{\mathbf{Y}}_{STA}(s)$ in (16). These two devices are parallel in each subsystem as shown in Fig. 3(b). Besides, the small-signal stability margin of these n subsystems is ranked in the order from smallest to largest, i.e.,

subsystem_{1,1}, subsystem_{1,2}, ..., and subsystem_{1,n}. We can see from Fig. 3(a) that the participation factor p_{1i} ($i=1, \dots, n$) determines the stability of the *critical* subsystem with given gSCR and dynamics of CBRs and STATCOMs. That is, if the participation factor p_{1i} of the CBR's dynamic (same as that of the subsystem_{1,1}) is larger, the *critical* subsystem will tend to be unstable; if the participation factor p_{1i} of the CBR's dynamic (same as that of the subsystem_{1,n}) is larger, the critical subsystem will be more stable. Since the participation factor p_{1i} ($i=1, \dots, n$) satisfy $0 < p_{1i} < 1$ ($i=1, \dots, n$), the extreme cases for the *critical* subsystem with given gSCR and dynamics of CBRs and STATCOMs are that: 1) when the participation factor p_{1i} of the CBR's dynamic (same as that of the subsystem_{1,1}) is one and the other p_{1i} are all zero (i.e., subsystem_{1,1}), the *critical* subsystem is most unstable; 2) when the p_{1i} of the CBR's dynamic (same as that of the subsystem_{1,n}) is one and the other p_{1i} are all zero (i.e., subsystem_{1,n}), the *critical* subsystem is most stable. That is, the small-signal stability of the *critical* subsystem (or the multi-CBR system with STATCOMs) is bounded by subsystem_{1,1} and subsystem_{1,n}, which will be further demonstrated in Section V.

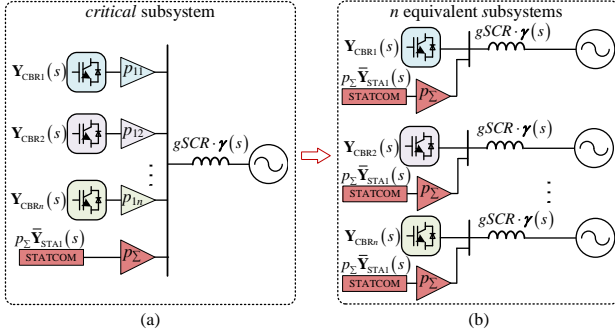


Fig. 3 Illustration of the *critical* subsystem and its equivalent subsystems: (a) the *critical* subsystem decoupled from the equivalent homogeneous system; (b) n equivalent subsystems of the *critical* subsystem.

C. Discussion of Key Impact Factors on System Stability

As described in Section III-A, for a multi-CBR system with STATCOMs, when the network parameters, and the control parameters of CBRs and STATCOMs are given, the varying operating conditions will cause the changes of CBRs' active power outputs P_{ei} , and STATCOMs' reactive current outputs I_{qsi} . In the following, we mainly discuss how these factors (P_{ei} and I_{qsi}) impact the small-signal stability from the viewpoint of grid strength and demonstrates the *critical* operating conditions, when the system tends to be most unstable.

1) The decrease of active power outputs P_{ei} , ($i=1, \dots, n$) increases gSCR and changes CgSCR. Since the sensitivity of gSCR for CBRs' active power outputs P_{ei} is negative^[22], the decrease of active power outputs of CBRs increases gSCR. Besides, as shown in (12), (17), and (19), the varying P_{ei} will change p_{1i} and p_{Σ} and thus changes CgSCR. Moreover, we can conclude that the decrease of P_{ei} increases p_{Σ} and thus increase the relative degree of the STATCOMs' impact on CgSCR. To be special, since the STATCOMs are commonly connected near the CBRs, we can approximately consider that STATCOMs are connected to CBRs' nodes. Due to this, the participation factor p_{Σ} can be approximately written as

$$p_{\Sigma} = \sum_{i=1}^n \frac{S_{Bsi}}{P_{ei}} p_{1i} \quad (20)$$

where S_{Bsi} , ($i=1, \dots, n$) are the capacities of STATCOMs, and satisfies $S_{Bsi} \geq 0$, wherein $S_{Bsi}=0$ means there is no STATCOMs near the node of CBR i ; p_{1i} is the participation factor satisfying $0 < p_{1i} < 1$ and $\sum_{i=1}^n p_{1i} = 1$. As shown in (20), the decrease of P_{ei} , ($i=1, \dots, n$) commonly increase p_{Σ} .

2) The reactive currents I_{qsi} , ($i=1, \dots, n$) only influence CgSCR, but has no impact on gSCR. As shown in (16) and (17), the varying reactive currents I_{qsi} , ($i=1, \dots, n$) mainly change the dynamics of the STATCOM $\bar{Y}_{STA1}(s)$ and thus influences CgSCR. Moreover, it is noteworthy that whether the increase of I_{qsi} increases or decreases CgSCR is uncertain, which depends on the dynamics of STATCOMs. This will be discussed in Section V.

3) The *critical* operating conditions are that all CBRs output rated active power (i.e., S_{Bi} , $i=1, \dots, n$), but the STATCOMs' reactive current outputs I_{qsi} ($i=1, \dots, k$) are uncertain in the multi-CBR system with STATCOMs. In other words, the *critical* operating conditions can be considered as that $gSCR = \lambda_{\min} \{S_B^{-1} B_{redn}\}$ in (9) and $I_{q\Sigma}$ in the range of $[-1, 1]$ for the

critical subsystem. We can conclude that the *critical* subsystem tends to be most unstable under *critical* operating conditions with the assumption that the connections of STATCOMs or $\bar{Y}_{STA}(s)$ decrease the CgSCR (or improve the system stability).

To be special, as discussed above in Section III-B, the decrease of CBRs' active power output increases p_{Σ} (i.e., the relative degree of the STATCOMs' impact on CgSCR). Therefore, when the STATCOMs decrease CgSCR, the decrease of CBRs' active power outputs causes the decrease of CgSCR due to that p_{Σ} increases. Besides, since the decrease of CBRs' active power output increases gSCR, (gSCR-CgSCR) becomes larger (i.e., the system becomes more stable) with the decrease of CBRs' active power outputs. That is, if the connection of STATCOMs decrease the CgSCR, the *critical* subsystem tends to be most unstable under *critical* operating conditions. We note that by experiments even that the connection of STATCOMs increases CgSCR, the system is likely to be most unstable under *critical* operating conditions, which will be shown in Section V.

Besides, we can conclude that the *critical* subsystem (or the original system) is robustly stable under varying operating conditions, if subsystem_{1,1}~subsystem_{1,n} in Fig. 3 are stable under *critical* operating conditions with the assumption that the connection of the STATCOM $\bar{Y}_{STA}(s)$ decrease the *critical* gSCR of subsystem_{1,1}~subsystem_{1,n} (named as CgSCR₁~CgSCR_n). The rationality of this assumption will be ensured in Section IV. To be special, as discussed above in Section III-B, the gSCR and p_{Σ} of subsystem_{1,1}~ subsystem_{1,n} are smallest under *critical* operating conditions in comparison with other operating conditions. Since the connection of STATCOM $\bar{Y}_{STA}(s)$ decreases CgSCR₁~CgSCR_n, the CgSCR₁~CgSCR_n are largest (due to that p_{Σ} is smallest) under *critical* operating conditions. Therefore, (gSCR-CgSCR_i) is smallest for each

subsystem_{1,i} under *critical* operating conditions. That is, subsystem_{1,1}~subsystem_{1,n} are most unstable under *critical* operating conditions with the assumption that the STATCOM $\bar{\mathbf{Y}}_{\text{STA}}(s)$ decrease CgSCR₁~CgSCR_n. Also due to that the stability of the *critical* subsystem is bounded by subsystem_{1,1}~subsystem_{1,n}, if subsystem_{1,1}~subsystem_{1,n} is stable under *critical* operating conditions with the above assumption, we can conclude that the *critical* subsystem (or the original system) is robustly stable under varying operating conditions.

IV. ADAPTIVE PARAMETER DESIGN OF STATCOMS UNDER VARYING OPERATING CONDITIONS

As discussed in Section III-C, the control design issue of the multi-CBR system with STATCOMs for robust small-signal stability under varying operating conditions can be simplified as that of subsystem_{1,1}~subsystem_{1,n} under *critical* operating conditions. Besides, since the CBRs are commonly black-boxed and thus it is hard to modify CBRs' control strategies in practical operations, we intend to modify STATCOMs' control strategies, which is more convenient. In this section, an adaptive control parameter design method for STATCOMs is proposed to ensure robust small-signal stability of subsystem_{1,1}~subsystem_{1,n} under *critical* operating conditions.

A. Adaptive Control Parameter Design Method for STATCOMs

\mathcal{H}_∞ -synthesis design is an efficient way to ensure the robust small-signal stability, which will be used for adaptive control-parameter design of STATCOMs. For brevity, we omit the detailed introduction of \mathcal{H}_∞ -synthesis design, which can refer to Ref. [18]. Based on the \mathcal{H}_∞ -synthesis method and the above analysis, the adaptive control parameter design problem of STATCOMs can be described as the simultaneous stabilization problem of subsystem_{1,1}~subsystem_{1,n} under *critical* operating conditions or a min-max optimization problem:

$$\min_{\mathbf{K}} \max_{\substack{i=1,\dots,n, I_{q\Sigma} \in [-1,1] \\ \text{gSCR}=\lambda_{\min}(\mathbf{S}_B^{-1}\mathbf{B}_{\text{redn}})}} \left\| \mathbf{C}_i (s\mathbf{I} - (\mathbf{A}_i + \mathbf{B}_i\mathbf{K}_i))^{-1} \mathbf{B}_i \right\|_{\infty} \quad (21)$$

where $\|\cdot\|_{\infty}$ is infinite norm; $\mathbf{C}_i (s\mathbf{I} - (\mathbf{A}_i + \mathbf{B}_i\mathbf{K}_i))^{-1} \mathbf{B}_i$ is the closed-loop transfer function matrix of subsystem_{1,i} under *critical* operating conditions; \mathbf{A}_i , \mathbf{B}_i , \mathbf{C}_i are parameter matrices of open-loop state-space model of subsystem_{1,i}, described as:

$$\text{subsystem}_{1,i} : \begin{cases} \dot{\mathbf{x}}_i = \mathbf{A}_i \mathbf{x}_i + \mathbf{B}_i \mathbf{u}_i \\ \mathbf{y}_i = \mathbf{C}_i \mathbf{x}_i \end{cases} \quad (22)$$

where \mathbf{x}_i , \mathbf{y}_i , and \mathbf{u}_i are vectors of state variables, algebraic variables, and input variables. Note that if the CBRs are "black-boxed", the parameter matrices \mathbf{A}_i , \mathbf{B}_i and \mathbf{C}_i can be obtained by identifying the internal dynamics through rational approximation based on frequency scan^[23]. \mathbf{K} in (21) represents the \mathcal{H}_∞ -controller in STATCOMs, which can be a transfer function matrix related with "s", or a static gain matrix. To simplify the difficulty of the adaptive parameter control design of STATCOMs, we do not change the original control structure of STATCOMs, and choose the proportional-integral (PI) parameters in AVC and PLL of STATCOMs as the elements in \mathbf{K} . That is, the matrix \mathbf{K} can be expressed as:

$$\mathbf{u}_i = \mathbf{K} \mathbf{y}_i, \mathbf{K} = \begin{bmatrix} k_{acps} & k_{acis} & 0 & 0 \\ 0 & 0 & k_{pllps} & k_{pllis} \end{bmatrix} \quad (23)$$

where $\mathbf{y}_i = [U_{qsi}, x_{1si}, (U_{si}-1), x_{2si}]^T$, wherein U_{qsi} and U_{si} are q -axis component and amplitude of STATCOM's terminal voltage in subsystem_{1,i}; x_{1si} and x_{2si} are the integrations of U_{qsi} and $(U_{si}-1)$; $\mathbf{u}_i = [\omega_{pll si}, I_{qref si}]^T$, wherein $\omega_{pll si}$ is the PLL's frequency output, and $I_{qref si}$ is the q -axis current reference; k_{acps} and k_{acis} are the PI parameters of AVC; k_{pllps} and $k_{pll is}$ are the PI parameters of PLL.

The optimization problem (21) is a pure-stabilization \mathcal{H}_∞ -synthesis problem, of which the necessary and sufficient condition is that the objective function in (21) is finite^[18]. Besides, if the objective function in (21) is smaller, the obtained control parameters of STATCOMs can improve the system's stability better. However, the range of the STATCOM's reactive current output $I_{q\Sigma}$ (i.e., $[-1, 1]$) is large in *critical* operating conditions. Due to this, the optimization problem (21) may have no solutions, which will be discussed in Section V. To deal with this issue, we divide the *critical* operating conditions as m sub-conditions. In these sub-conditions, $\text{gSCR} = \lambda_{\min} \{ \mathbf{S}_B^{-1} \mathbf{B}_{\text{redn}} \}$ and $I_{q\Sigma}$ is in the m intervals, i.e., $[-1, -1+2/m]$, $[-1+2/m, -1+4/m]$, ..., $[-1+2(m-1)/m, 1]$. For each sub-condition, we establish the corresponding optimization problem (21) and find the corresponding controller \mathbf{K}_i in (23) to ensure the robust small-signal stability of the n subsystems. In other words, to ensure the robust small-signal stability of the multi-CBR system with STATCOMs under varying operating conditions, we firstly obtain a set of controllers $\{\mathbf{K}_1, \dots, \mathbf{K}_m\}$ for STATCOMs by off-line solving established m optimization problems (21), and then on-line adaptively choose the proper controller \mathbf{K}_i according to the real-time reactive current outputs of all STATCOMs. Note that the experiments show that the obtained optimal controller \mathbf{K}_i can ensure to decrease CgSCR₁~CgSCR_n for subsystem_{1,1}~subsystem_{1,n}; besides, if m is larger, the \mathbf{K}_i can cause a larger decrease of CgSCR₁~CgSCR_n (or improve the system's stability better); but if m is too large, it will cause a high-computation demand; if m is too small or even equal to 1, the optimization problem (21) may have no solutions, which will be illustrated in Section V. Thus, m should be properly chosen to balance the control performance and computation cost.

B. Implementation Procedure of Proposed Control Method

As discussed above, the proposed adaptive control parameter design method of the multi-CBR system with STATCOMs under varying operating conditions mainly includes two parts: 1) Off-line calculate the control-parameter set $\{\mathbf{K}_1, \dots, \mathbf{K}_m\}$ for STATCOMs by solving the established m optimization problems (21), which is aimed to ensure the robust small-signal stability of subsystem_{1,1}~subsystem_{1,n} under m sub-conditions; 2) On-line adjust STATCOMs' control parameters based on the real-time reactive current outputs of STATCOMs and the control-parameter set $\{\mathbf{K}_1, \dots, \mathbf{K}_m\}$, which assumes that the real-time active power outputs of CBRs and reactive current outputs of STATCOMs can be obtained. The implementation

procedure of this proposed adaptive control parameter design method is shown in Fig. 4 with its main steps summarized as:

1) In off-line process, establish subsystem_{1,1}~subsystem_{1,n} for the multi-CBR system with STATCOMs under the *critical* operating conditions. If the inner parameters of CBRs are unknown, their internal dynamics can be identified by the rational approximation based on frequency scan^[23].

2) Establish m optimization problems (21) to ensure the small-signal stability of subsystem_{1,1}~subsystem_{1,n} under m sub-conditions, wherein m sub-conditions are obtained by dividing *critical* operating conditions. That is, $gSCR = \lambda_{\min}\{\mathbf{S}_B^{-1}\mathbf{B}_{redn}\}$ and $I_{q\Sigma}$ is in m intervals, i.e., $[-1, -1+2/m), [-1+2/m, -1+4/m), \dots, [-1+2(m-1)/m, 1]$.

3) Output control-parameter set $\{\mathbf{K}_1, \dots, \mathbf{K}_m\}$ obtained by solving m optimization problems (21) through Matlab solvers.

4) In on-line process, calculate real-time reactive current output $I_{q\Sigma}$ in (17).

5) On-line adjust the control parameters of STATCOMs based on the real-time $I_{q\Sigma}$ and control-parameter set $\{\mathbf{K}_1, \dots, \mathbf{K}_m\}$. To be special, if the real-time $I_{q\Sigma}$ is in the interval $[-1+2(i-1)/m, -1+2i/m)$, then the control parameters of all STATCOMs are set as \mathbf{K}_i , ($i=1, \dots, m$).

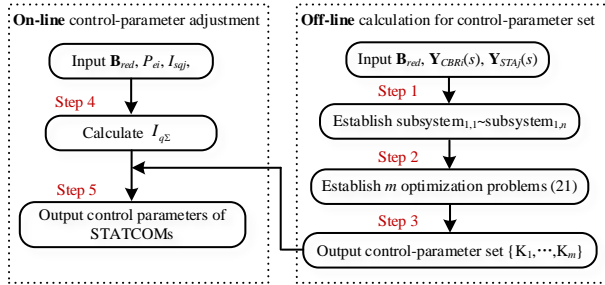


Fig. 4 Implementation procedure of the proposed adaptive control parameter design method for STATCOMs.

V. CASE STUDIES

In this section, the proposed grid-strength-based method and adaptive control parameter design method for a multi-CBR system with STATCOMs are validated by MATLAB/Simulink on a modified IEEE 39-node system as shown in Fig. 5, where nodes 1~9 are connected to CBRs through a set-up transformer, and node 39 is connected to external grids, simplified as an infinite bus. Each CBR represents a wind farm. The capacities of all CBRs refer to TABLE I. In practice, the wind farms are commonly installed with a certain percentage of STATCOMs for voltage support. Due to this, we install 30%-capacity STATCOM for each CBR located at high-voltage side in the modified 39-node system as shown in Fig. 5. The network parameters refer to Ref. [21]. Control parameters of CBRs and STATCOMs refer to TABLE II and TABLE III, respectively. Due to page limitation, we will focus on that the CBRs have different configurations or control parameters in the following simulations. That the CBRs are identical can be considered as a special case of a heterogeneous multi-CBR system.

A. Verification of Proposed GSCR-Based Method

The proposed gSCR-based method is first validated by eigenvalue analysis in the modified 39-node system in Fig. 5.

In this system, all STATCOMs are applied with the same AVC, and the CBRs are heterogeneous: CBR1~CBR3 are applied with constant active power control, the other CBRs are applied with dc voltage control, the PLL's PI parameters of CBR4~CBR6 are set as "13, 9800", and the PLL's PI parameters of other CBRs are set as "16, 9500". Several cases are created by decreasing the active power outputs of all CBRs from 1 to 0.5 p.u at the same proportion, which are normalized at their rated capacities. The corresponding gSCR increases from 1.68 to 3.36. Under these cases, we compare the resulting dominant eigenvalues of the modified 39-node system and its *critical* subsystem, as shown in Fig. 6 (a). The corresponding loci of the damping ratio of dominant eigenvalues for the modified 39-node system is given in Fig. 6 (b), which is represented by the red dotted curve.

TABLE I
RATED CAPACITIES OF EACH CBR (PER-UNIT)

CBR1	CBR2	CBR3	CBR4	CBR5
1	2	1	1	2
CBR6	CBR7	CBR8	CBR9	
10	2	2	1	

TABLE II
CONTROL PARAMETERS OF CBRs (PER-UNIT)

GFLCs	The PLL $H_{pll}(s)$	DC voltage loop $H_{dc}(s)$	Constant active power control loop $H_p(s)$
1~3	16+9500/s	/	1+5/s
4~6	13+9800/s	0.5+5/s	/
7~9	16+8500/s	0.5+5/s	/

Filter inductance L_f , filter capacitance C_f , dc capacitance C_{dc} : 0.05, 0.05, 0.038;
Transfer function of the current control loop $H_i(s)$: $1.5+10/s$;
Transfer function of the voltage feedforward control loop H_{ff} : $1/(1+0.0001s)$;
 q -axis current reference I_{qref} : 0.

TABLE III
CONTROL PARAMETERS OF STATCOMs (PER-UNIT)

Filter inductance L_{fs} , dc capacitance C_{dcs} : 0.1, 0.038;
Transfer function of current control loop $H_{is}(s)$: $1+10/s$;
Transfer function of dc voltage control loop $H_{dcs}(s)$: $1+5/s$;
Transfer function of the PLL $H_{plls}(s)$: $30+7000/s$;
Transfer function of the AVC $H_{avcs}(s)$: $1+5/s$

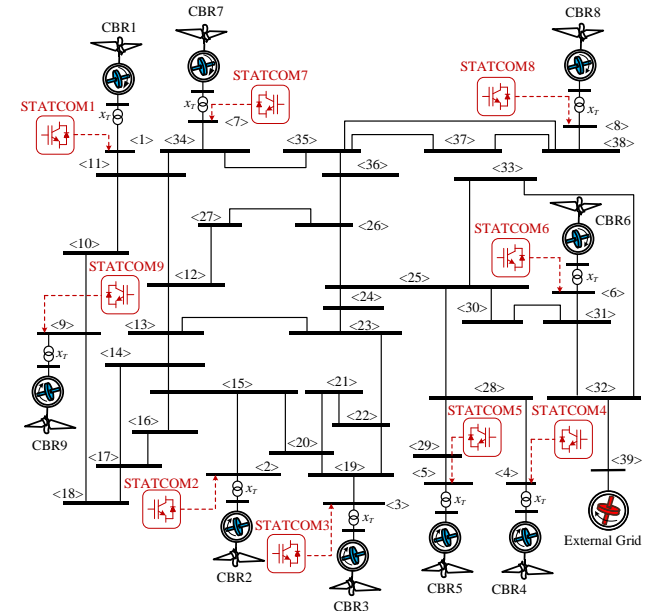


Fig. 5 A nine-CBR system with nine STATCOMs.

It can be seen from Fig. 6 (a) that the dominant eigenvalues of the *critical* subsystem match very well with the modified

39-node system, when the $gSCR$ is changed from 1.68 to 3.36. This indicates that the small-signal stability of the multi-CBR system with STATCOMs can be represented by that of the *critical* subsystem under varying operating conditions.

Moreover, Fig. 6 (a) shows that $gSCR$ can evaluate the small-signal stability of the modified 39-node system under varying operating conditions, when the control parameters of CBRs and STATCOMs are given. As shown in Fig. 6 (a), the $CgSCR$ is equal to 2.1. When $gSCR = CgSCR$, the system is critically stable; when $gSCR > CgSCR$, the system is stable; besides, the larger ($gSCR - CgSCR$) is, the more stable the system is; otherwise, if $gSCR < CgSCR$, the system is unstable. The same conclusion can also be observed from the loci of damping ratio of the system in Fig. 6 (b). The simulation results are consistent with the theoretical analysis in Section III.

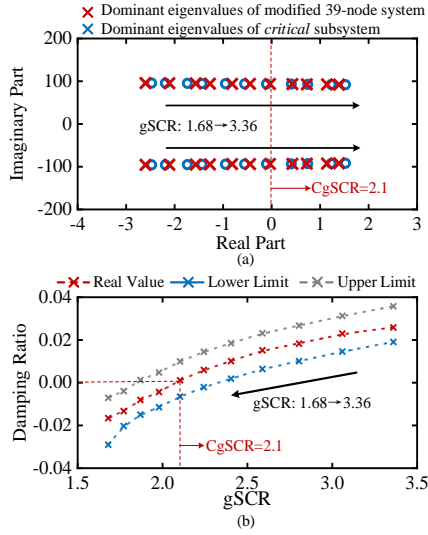


Fig. 6 when $gSCR$ changes from 1.68 to 3.36: (a) Loci of dominant eigenvalues of the modified 39-node system and *critical* subsystem; (b) Loci of damping ratio of dominant eigenvalues for the modified 39-node system (red dotted curve), weakest subsystem (blue dotted curve) and strongest subsystem (grey dotted curve)) in subsystem_{1,1} ~ subsystem_{1,9}.

Besides, it can be observed from Fig. 6 (b) that the small-signal stability of the multi-CBR system with STATCOMs is bounded by its upper and lower limits. According to the analysis in Section IV-B, the multi-CBR system with STATCOMs can be converted into an equivalent homogeneous system for small-signal stability analysis. The stability of the equivalent homogeneous system is bounded by subsystem_{1,1} and subsystem_{1,n}, which are corresponding to the most unstable and stable subsystems. Thus, the stability of the nine-CBR system with STATCOMs is bounded by the dynamics of subsystem_{1,1} and subsystem_{1,9}. In Fig. 6 (b), the blue and grey dotted curves are the loci of damping ratios of the subsystem_{1,1} and subsystem_{1,9}. Fig. 6 (b) shows that the red dotted curve is between the blue and grey dotted curves. This indicates that the modified 39-node system are bounded, which are consistent with the theoretical analysis in Section IV-B.

Furtherly, the electromagnetic time-domain simulation of the modified 39-node system is provided to verify the validity of the proposed $gSCR$ -based method. When the active power outputs of all CBRs are set as 0.7 and 0.9 p.u., the corresponding $gSCR$ are 2.404 and 1.87. Under these two cases,

a disturbance is applied to the infinite bus at $t=1s$ to cause 0.05 p.u. voltage drops and lasts 0.05s. The time-domain responses of the active power outputs of all CBRs under these two cases are given in Fig. 7.

It can be seen from Fig. 7 that when $gSCR = 2.404 > CgSCR$ (i.e., 2.1 as shown in Fig. 6), the system is stable. But when $gSCR = 1.87 < CgSCR$, the system is unstable. The time-domain simulation results are consistent with the eigenvalue analysis from Fig. 6, which verifies the effectiveness of the proposed $gSCR$ -based method.

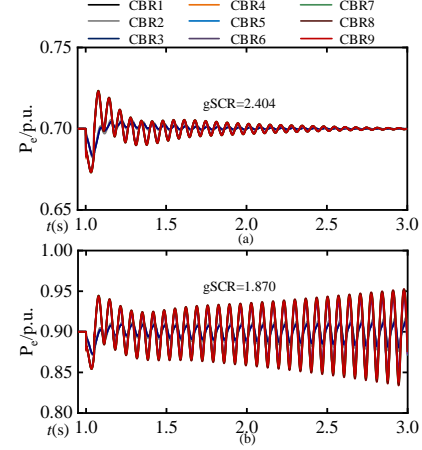


Fig. 7 Time-domain responses of the active power outputs of CBR1~CBR9: (a) $gSCR = 2.404$; (b) $gSCR = 1.87$.

B. Verification of Adaptive Control Parameter Design Method

The above subsection verifies that the small-signal stability of the multi-CBR system with STATCOMs under varying operating conditions is bounded by subsystem_{1,1} ~ subsystem_{1,n}. Besides, when the CBRs output rated active power, the system is most likely to be unstable as shown in Fig. 6. Therefore, the robust small-signal stability issues of the multi-CBR system with STATCOMs under varying operating conditions can be converted to that of subsystem_{1,1} ~ subsystem_{1,n} under *critical* operating conditions. Here, we furtherly verify the validity of the proposed adaptive control parameter design method for STATCOMs. Six scenarios are considered:

- 1) Divide *critical* operating conditions into 20 intervals;
- 2) Divide *critical* operating conditions into 10 intervals;
- 3) Divide *critical* operating conditions into 8 intervals;
- 4) Divide *critical* operating conditions into 4 intervals;
- 5) Divide *critical* operating conditions into 2 intervals;
- 6) Do not divide *critical* operating conditions.

The optimization problems (21) for these six scenarios are solved by Matlab solvers. The results for scenarios 1)~4) are given in TABLES. IV~VII. Note that the optimization problems (21) for scenarios 5)~6) have no solutions. This indicates that it may be hard to find fixed control parameters for STATCOMs to ensure the robust small-signal stability of the multi-CBR system with STATCOMs under all operating conditions. Therefore, it is necessary to adaptively adjustment STATCOMs' control parameters considering varying operating conditions.

Fig. 8 shows the $CgSCR$ of the *critical* subsystem under *critical* operating conditions for scenarios 1)~4), and the scenario that STATCOMs' control parameters refer to TABLE

III but PLL's PI parameters are set as 22, 7300 (as a reference), where the CgSCR are denoted as CgSCR₂₀, CgSCR₁₀, CgSCR₄ and CgSCR₀, respectively. Besides, the gSCR and CgSCR of the modified 39-node system without STATCOMs is 1.68 and 1.94, when the CBRs output rated active power. And the minimal value of CgSCR₁~CgSCR₉ for nine single-CBR infinite-bus systems with rated active power outputs is 1.57, wherein the CBR is one in the modified 39-node system.

TABLE IV

OPTIMAL CONTROL-PARAMETER SET FOR STATCOMs UNDER SCENARIO 1)					
$I_{q\Sigma}$	[-1, -0.9]	[-0.9, -0.8]	[-0.8, -0.7]	[-0.7, -0.6]	[-0.6, -0.5]
PLL	30.6+5796.4/s	28.5+5857.9/s	26.5+5915.0/s	24.4+5966.5/s	22.3+6009.7/s
AVC	2.75+5/s	2.77+5/s	2.79+5/s	2.81+5/s	2.83+5/s
$I_{q\Sigma}$	[-0.5, -0.4]	[-0.4, -0.3]	[-0.3, -0.2]	[-0.2, -0.1]	[-0.1, 0]
PLL	20.2+6040.5/s	18+6053.7/s	15.5+6020/s	12.8+6020/s	9.6+5547.3/s
AVC	2.85+5/s	2.88+5/s	2.91+5/s	2.91+5/s	2.98+5/s
$I_{q\Sigma}$	[0, 0.1]	[0.1, 0.2]	[0.2, 0.3]	[0.3, 0.4]	[0.4, 0.5]
PLL	5.1+3974.1/s	1+100/s	119.6+100/s	1+100/s	1+100/s
AVC	3.01+5/s	3.02+5/s	3.02+5/s	3.01+5/s	3.01+5/s
$I_{q\Sigma}$	[0.5, 0.6]	[0.6, 0.7]	[0.7, 0.8]	[0.8, 0.9]	[0.9, 1]
PLL	10.3+20000/s	9.2+14771.8/s	10+13302.9/s	11+12837.2/s	12.1+12582.9/s
AVC	2.93+5/s	2.86+5/s	2.79+5/s	2.71+5/s	2.64+5/s

TABLE V

OPTIMAL CONTROL-PARAMETER SET FOR STATCOMs UNDER SCENARIO 2)					
$I_{q\Sigma}$	[-1, -0.8]	[-0.8, -0.6]	[-0.6, -0.4]	[-0.4, -0.2]	[-0.2, 0]
PLL	29.5+5791.6/s	25.3+5902.2/s	21+5974.7/s	16.3+5942.2/s	10.2+5381.8/s
AVC	2.79+5/s	2.82+5/s	2.86+5/s	2.92+5/s	2.99+5/s
$I_{q\Sigma}$	[0, 0.2]	[0.2, 0.4]	[0.4, 0.6]	[0.6, 0.8]	[0.8, 1]
PLL	1+100/s	119.6+100/s	97.8+100/s	9.2+14726.5/s	11.1+12831.5/s
AVC	3.02+5/s	3+5/s	2.97+5/s	2.85+5/s	2.7+5/s

TABLE VI

OPTIMAL CONTROL-PARAMETER SET FOR STATCOMs UNDER SCENARIO 3)					
$I_{q\Sigma}$	[-1, -0.75]	[-0.75, -0.5]	[-0.5, -0.25]	[-0.25, 0]	[0, 0.25]
PLL	28.9+5785.7/s	23.6+5909.5/s	17.9+5927.3/s	10.5+5316.3/s	1+100/s
AVC	2.8+5/s	2.84+5/s	2.91+5/s	2.99+5/s	3.02+5/s
$I_{q\Sigma}$	[0.25, 0.5]	[0.5, 0.75]	[0.75, 1]		
PLL	105.2+100/s	10.3+20000/s	10.5+13036/s		
AVC	2.98+5/s	2.92+5/s	2.74+5/s		

TABLE VII

OPTIMAL CONTROL-PARAMETER SET FOR STATCOMs UNDER SCENARIO 4)					
$I_{q\Sigma}$	[-1, -0.5]	[-0.5, 0]	[0, 0.5]	[0.5, 1]	
PLL	25.8+5701.1/s	12.2+4900.7/s	1+100/s	10.9+20000/s	
AVC	2.87+5/s	3+5/s	3.02+5/s	2.9+5/s	

As shown in Fig. 8, when the STATCOM uses the control parameters in TABLE III with PLL's PI parameters as 22, 7300, the CgSCR may be larger (or smaller) than 1.94, i.e., the connection of STATCOMs may deteriorate (or improve) system stability. Besides, the increase of STATCOM's reactive current output $I_{q\Sigma}$ may increase or decrease the CgSCR (i.e., deteriorate or improve the stability). These indicate that the impact of the connection of STATCOMs and varying $I_{q\Sigma}$ on the CgSCR (or the system stability) is uncertain, which depends on the dynamics of STATCOMs. Moreover, the increase of $I_{q\Sigma}$ may cause CgSCR>gSCR=1.68, i.e., the system becomes unstable. This demonstrates the necessity to dynamically adjust STATCOMs' control parameters to ensure the robust small-signal stability of the multi-CBR system with STATCOMs under varying operating conditions. In comparison, we can see from Fig. 8 that the CgSCR of the *critical* subsystem under scenarios 1)~4) are always smaller than 1.5 (smaller than 1.68 and 1.57), when $I_{q\Sigma}$ is in the range of

[-1,1]. That is, the obtained control parameters set for STATCOMs can ensure the robust small-signal stability of the *critical* subsystem and that the STATCOM decreases CgSCR₁~CgSCR₉ (improves the stability of subsystem_{1,1}~subsystem_{1,n}) under *critical* operating conditions. This illustrates that the proposed adaptive control parameter design method for STATCOMs can ensure the robust small-signal stability of the multi-CBR system with STATCOMs under varying operating conditions. Besides, we can see that the red and blue curves are commonly smaller than the brown and grey curves. This demonstrates that when the divided sub-conditions are more, the obtained STATCOMs' control-parameter set can improve the system stability better.

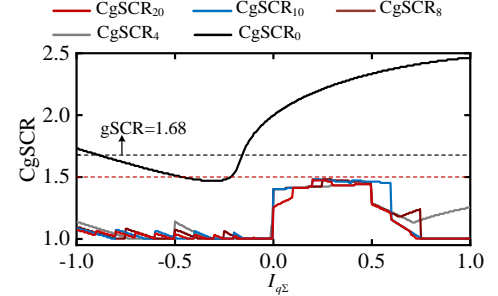


Fig. 8 CgSCR for the *critical* subsystem under *critical* operating conditions for scenarios 1)~4) and the scenario that control parameters of STATCOMs refer to TABLE III, but PLL's PI parameters are 22, 7300.

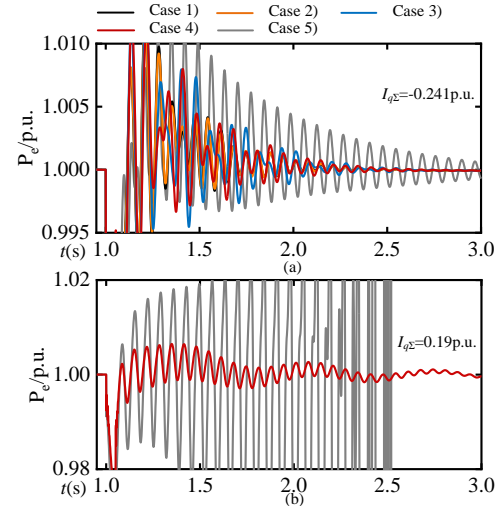


Fig. 9 Time-domain responses of CBR1's active power output with STATCOMs' control parameters under different scenarios: (a) the equivalent $I_{q\Sigma}=-0.241$ p.u.; (b) the equivalent $I_{q\Sigma}=0.19$ p.u..

Furtherly, the electromagnetic time-domain simulation of the modified 39-node system is provided to verify the proposed control method. Two operating conditions are considered: 1) all CBRs output rated active power and the equivalent reactive current $I_{q\Sigma}=-0.241$ p.u.; 2) all CBRs output rated active power and the equivalent reactive current $I_{q\Sigma}=0.19$ p.u.. For each operating condition, we consider 5 cases:

- 1) All STATCOMs use control parameters in TABLE IV;
- 2) All STATCOMs use control parameters in TABLE V;
- 3) All STATCOMs use control parameters in TABLE VI;
- 4) All STATCOMs use control parameters in TABLE VII;
- 5) All STATCOMs use the control parameters in TABLE III, but PLL's PI parameters are set as 22, 7300, as a reference.

For each case, a disturbance is applied to the infinite bus at $t=1s$ to cause 0.05 p.u. voltage drops and lasts 0.05s. The time-domain responses of the active power outputs of CBR1 for these cases are given in Fig. 9. In Fig. 9 (b), since the control parameters of STATCOMs in TABLE IV~TABLE VII are the same when $I_{q\Sigma}=0.19$ p.u., we only give the responses of CBR1's active power output under one of cases 1)~4). We can see from Fig. 9 that the system is robustly stable under different $I_{q\Sigma}$, when the STATCOMs are based on the proposed adaptive control; but the system changes from stability to instability with fixed STATCOMs' control parameters, when $I_{q\Sigma}$ changes from -0.241 to 0.19 p.u.. The simulation results are consistent with the analysis by Fig. 8 and thus verify the validity of the proposed adaptive control parameter design method for STATCOMs.

VI. CONCLUSIONS

In this paper, an adaptive control-parameter design method for STATCOMs was proposed to ensure the robust small-signal stability of a multi-CBR system with STATCOMs considering varying operating conditions. Firstly, we proposed a grid-strength-based method for evaluating small-signal stability of the multi-CBR system with STATCOMs under varying operating conditions. This proposed grid-strength-based method can simplify the multi-CBR system with STATCOMs as multiple subsystems for small-signal stability analysis, which can avoid establishing the detailed dynamical model of the original system. Based on the grid-strength-based method, we found the *critical* operating conditions, where the system tends to be most unstable. Due to this, we converted the robust small-signal stability issues of the multi-CBR with STATCOMs as that of multiple subsystems under *critical* operating conditions, which can avoid considering all operating conditions. Moreover, based on the H_∞ control theory, we proposed an adaptive control-parameter design method for STATCOMs to ensure the robust stability of the multiple subsystems under *critical* operating conditions. In the proposed control method, we established a control-parameter set for STATCOMs off-line, and dynamically adjustment control parameters of STATCOMs on-line through the obtained control-parameter set and real-time reactive current outputs of STATCOMs. The proposed control method can ensure the robust small-signal stability of the multi-CBR system with STATCOMs under varying operating conditions. The effectiveness of the proposed grid-strength-based method and adaptive control parameter design method were verified in a nine-CBR system with nine STATCOMs. In our future works, we will explore how to coordinate the CBRs and STATCOMs with other devices (e.g., energy storage devices and static var capacitors, SVC) to ensure the robust small-signal stability of the system under varying operating conditions.

REFERENCES

- [1] Q. Peng, Q. Jiang, H. Yang, T. Liu, H. Wang, and F. Blaabjerg, "On the stability of power electronics-dominated systems: challenges and potential solutions," *IEEE Trans. Ind. Appl.*, vol. 55, no. 6, pp. 7657–7670, Nov. 2019.
- [2] F. Milano, F. Dörfler, G. Hug, D. J. Hill, and G. Verbić, "Foundations and challenges of low-inertia systems," in *2018 Power Systems Computation Conference (PSCC)*. IEEE, pp. 1–25, 2018.
- [3] Y. Cheng, L. Fan, and et al., "Real-world subsynchronous oscillation events in power grids with high penetrations of inverter-based resources," *IEEE Trans. Power Systems*, vol. 38, no. 1, pp. 316–330, Jan. 2023.
- [4] H. Liu, X. Xie, and et al., "Subsynchronous interaction between direct-drive PMSG based wind farms and weak AC networks," *IEEE Trans. Power syst.*, vol. 32, no. 6, pp. 4708–4720, Nov. 2017.
- [5] J. Hu, B. Wang, and et al., "Small signal dynamics of DFIG-based wind turbines during riding through symmetrical faults in weak ac grid," *IEEE Trans. Energy Convers.*, vol. 32, no. 2, pp. 720–730, Jun. 2017.
- [6] P. Sun, J. Yao, and et al., "Virtual capacitance control for improving dynamic stability of the DFIG-based wind turbines during a symmetrical fault in a weak ac grid," *IEEE Trans. Ind. Electron.*, vol. 68, no. 1, pp. 333–346, Jan. 2021.
- [7] D. Zhu, S. Zhou, X. Zou, and et al., "Small-signal disturbance compensation control for LCL-type grid-connected converter in weak grid," *IEEE Trans. Ind. Appl.*, vol. 56, no. 3, May, 2020.
- [8] X. Tian, Y. Chi, and et al., "Coordinated damping optimization control of sub-synchronous oscillation for DFIG and SVG," *CSEE Journal of Power and Energy Systems*, vol. 7, no. 1, pp. 140–149, Jan. 2021.
- [9] Y. Zhang, Y. Yang, X. Chen, and et al., "Intelligent parameter design-based impedance optimization of STATCOM to mitigate resonance in wind farms," *IEEE J. Emerg. Sel. Topics Power Electron.*, vol. 9, no. 3, pp. 3201–3215, Jun. 2021.
- [10] H. Yuan, H. Xin, and et al., "Small-signal stability assessment of multi-converter-based-renewable systems with STATCOMs based on generalized short-circuit ratio," *IEEE Trans. Energy Convers.*, vol. 37, no. 4, pp. 2889–2902, Dec. 2022.
- [11] L. Fan, "Modeling type-4 wind in weak grids," *IEEE Trans. Sustain. Energy*, vol. 10, no. 2, pp. 853–864, Apr. 2019.
- [12] M. Cespedes and J. Sun, "Impedance modeling and analysis of grid-connected voltage-source converters," *IEEE Trans. Power Electron.*, vol. 29, no. 3, pp. 1254–1261, Mar. 2014.
- [13] C. Zhang, X. Cai, A. Rygg, and M. Molinas, "Sequence domain SISO equivalent models of a grid-tied voltage source converter system for small-signal stability analysis," *IEEE Trans. Energy Convers.*, vol. 33, no. 2, pp. 741–749, Jun. 2018.
- [14] L. Xu, H. Xin, L. Huang and et al., "Symmetric admittance modeling for stability analysis of grid-connected converters," *IEEE Trans. Energy Convers.*, vol. 35, no. 1, pp. 434–444, Mar. 2020.
- [15] Y. Liao, X. Wang, "Impedance-based stability analysis for interconnected converter systems with open loop RHP poles," *IEEE Trans. Power Electron.*, vol. 35, no. 4, pp. 4388–4397, Apr. 2020.
- [16] L. Huang, H. Xin, Z. Li, and et al., "Grid-synchronization stability analysis and loop shaping for PLL-based power converters with different Reactive power control," *IEEE Trans. Smart Grid*, vol. 11, no. 1, pp. 501–516, Jan. 2020.
- [17] G. Li, Y. Chen, A. Luo and et al., "An enhancing grid stiffness control strategy of STATCOM/BESS for damping sub-synchronous resonance in wind farm connected to weak grid," *IEEE Trans. Ind. Informat.*, vol. 16, no. 9, pp. 5835–5845, Sep. 2020.
- [18] P. Apkarian, D. Noll, "Nonsmooth H_∞ Synthesis," *IEEE Trans. Autom. Control*, vol. 51, no. 1, pp. 71–86, Jan. 2006.
- [19] Y. Zhou, G. Wang, et al., "Small-signal Stability Analysis of Power Systems under Uncertain Renewable Generation," *2022 IEEE Power & Energy Society General Meeting (PESGM)*, Denver, CO, USA, 2022.
- [20] H. Yuan, X. Qin, and et al., "Small Signal Stability Analysis of Grid-Following Inverter-Based Resources in Weak Grids With SVGs Based on Grid Strength Assessment," *2021 IEEE 1st International Power Electronics and Application Symposium (PEAS)*, Shanghai, China, 2021.
- [21] L. Huang, H. Xin, W. Dong, and F. Dörfler, "Impacts of grid structure on PLL-synchronization stability of converter-integrated power systems," *arXiv preprint arXiv:1903.05489*, 2019.
- [22] H. Liang, et al., "Optimal Capacity Allocation of Renewable Energy Generation Base for Small Signal Stability Improvement," *2019 IEEE Innovative Smart Grid Technologies - Asia (ISGT Asia)*, Chengdu, China, 2019, pp. 1772–1776.
- [23] B. Gustavsen and A. Semlyen, "Rational approximation of frequency domain responses by vector fitting," *IEEE Transactions on Power Delivery*, vol. 14, no. 3, pp. 1052–1061, 1999.